
BioDiffusion: A Versatile Diffusion Model for Biomedical Signal Synthesis

Xiaomin Li ¹, Mykhailo Sakevych ¹, Gentry Atkinson ², and Vangelis Metsis ¹
Texas State University¹ xminli, ukb12, vmetsis@txstate.edu
St. Edwards University² gatkinso@stedwards.edu

Abstract

Machine learning tasks involving biomedical signals frequently grapple with issues such as limited data availability, imbalanced datasets, labeling complexities, and the interference of measurement noise. These challenges often hinder the optimal training of machine learning algorithms. Addressing these concerns, we introduce BioDiffusion, a diffusion-based probabilistic model optimized for the synthesis of multivariate biomedical signals. BioDiffusion demonstrates excellence in producing high-fidelity, non-stationary, multivariate signals for a range of tasks including unconditional, label-conditional, and signal-conditional generation. Leveraging these synthesized signals offers a notable solution to the aforementioned challenges. Our research encompasses both qualitative and quantitative assessments of the synthesized data quality, underscoring its capacity to bolster accuracy in machine learning tasks tied to biomedical signals. Furthermore, when juxtaposed with current leading time-series generative models, empirical evidence suggests that BioDiffusion outperforms them in biomedical signal generation quality.

Source code link: [Link](#).

1 Introduction

The significance of biomedical signal processing is continually emphasized in its role across various ubiquitous computing applications. The quest for accurate,

dependable data has been a driving force for innovations that lead to improved assistive technologies and deeper insights into diagnostics, patient monitoring, and therapeutics. Electrocardiograms (ECGs), electroencephalograms (EEGs), and data from human activity sensors represent a treasure trove of information. Their analysis has ushered in transformative breakthroughs, but not without associated challenges.

One major hurdle faced by biomedical signal processing is the intricacies that arise due to limited dataset size, imbalances in datasets, artificial noise, and anomalies. These factors can critically compromise the performance of machine learning models, necessitating the development of innovative solutions. Historically, approaches like data augmentation, data resampling, and statistical analyses have been employed to mitigate these challenges. Yet, the inherently non-stationary and multivariate characteristics of biomedical signals add another layer of complexity. Encouragingly, recent research trends highlight an uptick in leveraging deep learning for enhancing the preprocessing of biomedical signals [9, 20, 21].

Deep learning, though powerful, is often constrained by the nuances of biomedical datasets. Recognizing these challenges, our study introduces the BioDiffusion model, a diffusion-based probabilistic approach tailored for biomedical signal generation. Designed to adeptly handle a plethora of generation tasks, BioDiffusion serves as a holistic solution to biomedical signal synthesis challenges. From expanding training dataset sizes to anomaly removal and super-resolution, our model's adaptability offers a promising avenue for more efficient and precise analysis techniques in clinical applications.

Inspired by the Stable Diffusion model's prowess in image synthesis [19], we've adapted the BioDiffusion model to resonate with the unique traits of biomedical signals. To evaluate our model, we've engaged in a multi-faceted assessment, employing visual similarity comparisons, dimension reduction technologies like UMAP [13], and similarity scores such as wavelet

coherence. Additionally, our research delves into the synthesis signals’ potential in machine learning model training, juxtaposing synthetic signals against real signals.

Through rigorous benchmarking against contemporary time-series synthesis models, our findings illuminate the BioDiffusion model’s superior proficiency in generating high-fidelity biomedical signals. The implications of our proposed model are profound; it presents a significant stride toward enhancing diagnostics, patient monitoring, and advancing biomedical research.

Main Contributions:

- Presentation of the BioDiffusion model, our innovative diffusion-based probabilistic approach tailored to address the complexities inherent in biomedical signal generation.
- Demonstration of our model’s versatility in handling diverse generation tasks, presenting a unified solution to biomedical signal synthesis.
- Comprehensive evaluation of the BioDiffusion model through both qualitative and quantitative metrics, underscoring its effectiveness and precision.
- Comparative analysis highlighting the superior capability of BioDiffusion in biomedical signal synthesis relative to existing state-of-the-art models.

The remainder of this paper is structured as follows: Section 2 delves into pertinent works related to signal synthesis. Section 3 elucidates the BioDiffusion model’s methodology and its specific adaptations for biomedical signals. Section 4 presents our experimental framework, datasets, evaluation metrics, and a comparative analysis with other models, underlining BioDiffusion’s standout performance. Finally, Section 5 rounds off the paper, encapsulating the salient points and suggesting avenues for future exploration.

2 Related Work

This section delves into the pertinent literature in the realms of generative models and diffusion models for signal synthesis. Our objective is to offer a comprehensive perspective on their evolution, strengths, and constraints, especially in the context of time-series signal synthesis.

2.1 Generative Models in Signal Synthesis

Generative models aim to discern the inherent structure of data, enabling the generation of new samples

mirroring the original data. Several paradigmatic approaches within generative models for time-series synthesis include:

- **Generative Adversarial Networks (GANs):** Comprising two adversarial networks—the generator and the discriminator—GANs aim for the generator to improve its synthetic data samples to deceive the discriminator. Their prowess extends to various data types including time-series signals. Notable implementations include the transformer-based GAN by Xiaomin L. et al. [11] which sets a benchmark for synthetic time-series signal fidelity, TimeGAN by Jinsung Y. et al. [28] tailoring GANs for realistic time-series data, and the Recurrent Conditional GAN (RCGAN) by Cristóbal E. et al. [2] for time-series generation. Despite their proficiency in crafting realistic samples, GANs can exhibit training instability and suffer from mode collapse.
- **Variational Autoencoders (VAEs):** VAEs, through their encoder-decoder architecture, learn a probabilistic representation of data. Works such as that by Vincent F. et al. [3] exploit VAEs for imputing missing multivariate time-series values, while Fu et al. [4] leverage VAEs for augmenting time-series in human activity recognition. VAEs offer more consistent training than GANs but may produce less diverse samples, contingent on latent space distribution choices.
- **Autoregressive Models:** These models sequentially generate samples, with each new element contingent on prior elements. WaveNet by Aaron van den Oord et al. [18] exemplifies this, producing raw audio waveforms using dilated causal convolutions for long-range temporal relationship capture. Although proficient in modeling temporal dynamics, their sequential nature can be computationally slow and may falter in grasping extended dependencies.
- Other generative paradigms like **Normalizing Flows**, **Restricted Boltzmann Machines (RBMs)**, and **Non-negative Matrix Factorization (NMF)** have been explored. However, their efficacy diminishes with multidimensional non-stationary time-series signals.

2.2 Diffusion Models for Time-series Synthesis

Diffusion models harness latent variables to understand a dataset by modeling data point propagation through latent space. They function by adding Gaussian noise to training data (forward diffusion) and

subsequently reversing this process (reverse diffusion) to retrieve the data [27]. Their prowess has been manifested in diverse arenas like image synthesis and molecule design [26].

Several prominent studies in diffusion models include:

- Yang L. et al.’s comprehensive discourse on deep learning-based diffusion models and their applicability to time-series tasks [27].
- Garnier O. et al. augmenting diffusion models for infinite-dimensional spaces, targeting audio signals and time series [6].
- Kong et al.’s exploration into audio synthesis through diffusion models [10] and Tashiro et al.’s venture into time-series imputation [25].
- Alcaraz et al.’s pursuit of time-series forecasting using diffusion models [1].

While these studies accentuate the capabilities of generative and diffusion models for time-series synthesis, there remain challenges in terms of scalability, stability, and fidelity, especially for intricate biomedical signals. Our proposed BioDiffusion model stands as an endeavor to surmount these challenges, deriving inspiration from prior works while innovating for enhanced versatility and efficacy in biomedical signal synthesis. The forthcoming section elucidates the methodology underlying BioDiffusion, illustrating its potential to revolutionize biomedical signal synthesis.

3 Diffusion Probabilistic Models

This section provides an overview of diffusion models, their extension to conditional data generation, and associated neural architectures.

Diffusion models [23, 8] consist of a forward process that iteratively degrades data $\mathbf{x}_0 \sim q(\mathbf{x}_0)$ by adding Gaussian noise over T iterations:

$$q(\mathbf{x}_t | \mathbf{x}_{t-1}) = \mathcal{N}\left(\mathbf{x}_t; \sqrt{1 - \beta_t} \mathbf{x}_{t-1}, \beta_t \mathbf{I}\right), \quad (1)$$

$$q(\mathbf{x}_{1:T} | \mathbf{x}_0) = \prod_{t=1}^T q(\mathbf{x}_t | \mathbf{x}_{t-1}). \quad (2)$$

The reverse process incrementally restores the noise-corrupted data:

$$p_\theta(\mathbf{x}_{t-1} | \mathbf{x}_t) = \mathcal{N}(\mathbf{x}_{t-1}; \boldsymbol{\mu}_\theta(\mathbf{x}_t, t), \boldsymbol{\Sigma}_\theta(\mathbf{x}_t, t)), \quad (3)$$

$$p_\theta(\mathbf{x}_{0:T}) = p(\mathbf{x}_T) \prod_{t=1}^T p_\theta(\mathbf{x}_{t-1} | \mathbf{x}_t). \quad (4)$$

The forward process hyperparameters β_t are set such that \mathbf{x}_T approximates a standard normal distribution. The reverse process optimizes the evidence lower bound (ELBO) [5], with the loss given by:

$$L_\theta(\mathbf{x}_0) = \mathbb{E}_q \left[L_T(\mathbf{x}_0) + \sum_{t>1} D_{\text{KL}}(q(\mathbf{x}_{t-1} | \mathbf{x}_t, \mathbf{x}_0) \| p_\theta(\mathbf{x}_{t-1} | \mathbf{x}_t)) - \log p_\theta(\mathbf{x}_0 | \mathbf{x}_1) \right], \quad (5)$$

where $L_T(\mathbf{x}_0) = D_{\text{KL}}(q(\mathbf{x}_T | \mathbf{x}_0) \| p(\mathbf{x}_T))$.

Following prior work [23, 8], the reverse process parameters are:

$$\begin{aligned} \boldsymbol{\mu}_\theta(\mathbf{x}_t, t) &= \frac{1}{\sqrt{\alpha_t}} \left(\mathbf{x}_t - \frac{\beta_t}{\sqrt{1 - \bar{\alpha}_t}} \boldsymbol{\epsilon}_\theta(\mathbf{x}_t, t) \right), \quad (6) \\ \boldsymbol{\Sigma}_\theta^{ii}(\mathbf{x}_t, t) &= \exp \left(\log \tilde{\beta}_t + \left(\log \beta_t - \log \tilde{\beta}_t \right) v_\theta^i(\mathbf{x}_t, t) \right), \quad (7) \end{aligned}$$

with $\alpha_t = 1 - \beta_t$, $\bar{\alpha}_t = \prod_{s=1}^t \alpha_s$, and $\tilde{\beta}_t = \frac{1 - \bar{\alpha}_t - 1}{1 - \bar{\alpha}_t} \beta_t$.

Improved sample quality is achieved by optimizing modified losses, resembling denoising score matching over multiple noise levels [24, 8].

A critical aspect of diffusion models is the extension to conditional data generation, wherein both the data \mathbf{x}_0 and a set of conditions \mathbf{c} are incorporated. The conditions can be any additional information or constraints provided externally, influencing the generative process. By assimilating \mathbf{c} , the reverse process becomes:

$$p_\theta(\mathbf{x}_{t-1} | \mathbf{x}_t, \mathbf{c}) \mathcal{N}(\mathbf{x}_{t-1}; \boldsymbol{\mu}_\theta(\mathbf{x}_t, t, \mathbf{c}), \boldsymbol{\Sigma}_\theta(\mathbf{x}_t, t, \mathbf{c})). \quad (8)$$

Intuitively, \mathbf{c} offers an avenue to guide the generative model, providing a degree of control over the outputs. This inclusion makes diffusion models versatile, catering to scenarios like content-specific image generation or style-conditioned audio synthesis.

For the architecture, we employ a feed-forward neural network. It has distinct input layers for data, the conditions \mathbf{c} , and the time step. In line with the approach in [12], our model leverages multi-scale structures through convolutional layers, enabling the extraction of hierarchical information. The training strategy employs early stopping, hinging on the validation set ELBO to prevent overfitting.

3.1 Unconditional Diffusion Models

The unconditional diffusion model employs a Markov chain-based generation process, converting data iteratively between its original form and noise. This intricate transformation is portrayed in Figure 1.

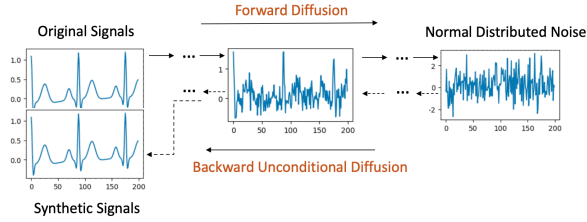


Figure 1: Unconditional Diffusion process

Forward Process: Starting with the original signal, it is incrementally perturbed with Gaussian noise over a series of diffusion steps, spanning $[0, T]$. By the end of step T , the resulting signal retains the dimensions of the original but its data values adopt a normal distribution.

Backward Process: Initiating this process, signals derived from Gaussian noise serve as inputs at diffusion step T . As the model retraces the steps back to 0, it methodically diminishes the noise. Each step t consumes the previous step’s output ($t + 1$) as its input. A crucial aspect during this phase is the evaluation of the KL divergence between signals at the corresponding steps in both the forward and backward processes. The objective is to minimize this divergence. When the backward process culminates at step 0, the signals generated should closely mirror the original ones.

Signal Generation: Post-training, the model is equipped to accept random Gaussian noise. By invoking the backward process, it can craft synthetic signals. This procedure is dubbed "unconditional" due to the absence of stipulations on the signal generation from the noise. Such a design empowers the diffusion model to assimilate the dataset’s entire distribution, endowing it with the capability to potentially produce any signal within the dataset’s feature space.

3.2 Label Conditional Diffusion Models

Label-conditional diffusion models extend the framework of their unconditional counterparts by integrating scalar labels with each input datum. This inclusion of labels not only shapes the diffusion process but also allows for more targeted synthesis of signals, as elaborated below.

Forward Process with Labels: In this process, as depicted in Fig. 2, original signals are systematically associated with their corresponding labels. Within the U-Net architecture (detailed in section 3.4), each residual block is enriched with both the scalar label and the ongoing diffusion timestep, leveraging an embedding technique.

Backward Process with Labels: Here, the diffu-

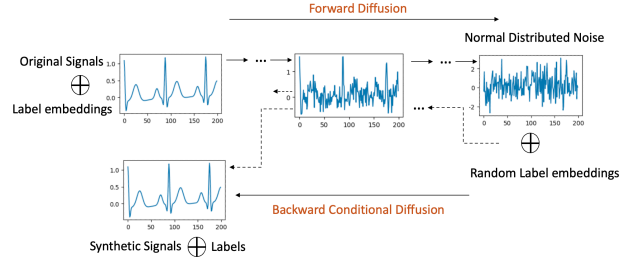


Figure 2: Label Conditional Diffusion process

sion model ingests noise, drawn from a normal distribution, in tandem with a designated label. As the model progresses through the diffusion steps, there’s a persistent focus on quantifying and minimizing the KL divergence between the signals emerging from the forward and backward processes.

Synthetic Signal Generation: The culmination of this methodology is a trained diffusion model possessing dual capabilities. It is not only attuned to the holistic data distribution of the dataset but is also adept at crafting synthetic signals pertinent to a delineated class.

3.3 Signal Conditional Diffusion Models

Signal-conditional diffusion models, visualized in Fig. 3, introduce a nuanced methodology where signal conditions play a pivotal role exclusively during the backward diffusion phase, differentiating it from label-conditional approaches.

Forward Process: The forward diffusion process in the case of signal conditioning is the same as the original, unconditional diffusion.

Backward Diffusion with Signal Conditioning: For the backward phase, a perturbed signal forms the conditional input, which could stem from an original signal sample tainted by noise, artifacts, or even be a downsampled version mirroring the original signal’s dimensions. This conditional signal is amalgamated with noise drawn from a normal distribution. Post this combination, a convolutional layer refines it to align with the original signal’s structure. The remainder of the backward process strives to cleanse the noise and produce a clean signal resembling the original signal it was seeded with.

3.4 U-Net Architecture

The U-Net architecture (see Figure 4) is used in each diffusion process pipeline. We modify the model depicted in the work [22] to fit for time-series signals instead of $N \times N$ images. The signals in time step \mathbf{x}_t are concatenated with the time step embeddings and other

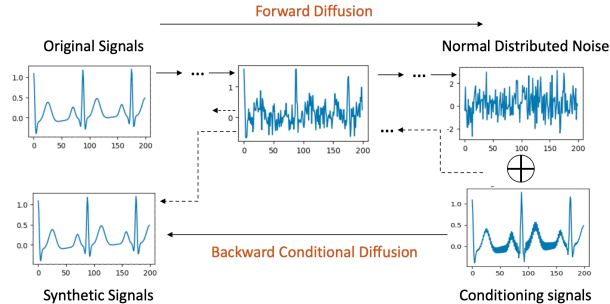


Figure 3: Signal Conditional Diffusion process

conditional embeddings (low-quality signals or labels) input to the U-Net model, and the U-Net model generates signals in time $t - 1$. We repeat this process from $t = T$ till $t = 0$ to train the U-Net model.

4 Experimental Results

This section delves into the various methodologies employed by diffusion models in the synthesis of biomedical signals. We’ve partitioned our approach into three categories: unconditional, label-conditional, and signal-conditional diffusion processes. Our qualitative and quantitative evaluations underscore the efficacy of the generated synthetic data. We also benchmark our findings against state-of-the-art methods, underscoring the advantages of our model and pinpointing areas ripe for further refinement. We aim to demonstrate that diffusion models are promising candidates for crafting high-caliber biomedical signals, potentially transforming myriad biomedical arenas.

4.1 Datasets

Our model’s performance is gauged across three datasets: a simulated one, the UniMiB human activity recognition (HAR) dataset [14], and the MIT-BIH Arrhythmia Database [16, 7].

- **Simulated Dataset:** Comprising synthetic signals with patterns like bell, funnel, and cylinder shapes, this dataset contains five classes each defined by attributes such as amplitude and pattern variances. Each signal has 512 timesteps and is unidimensional. Its primary purpose is to assess the diffusion model’s adaptability on simplified data.
- **UniMiB Dataset** [14]: Derived from smartwatches, this dataset has nine human activity classes with each signal capturing 151 timesteps across three acceleration dimensions. Adapted to our U-Net architecture, signals have been resized to 128 timesteps. The training set contains

6055 samples, with class distributions that peak at 1572 and trough at 119 samples per class. The test set has 1524 samples, ranging from 32 to 413 samples per class, highlighting the dataset’s imbalance.

- **MIT-BIH Arrhythmia Dataset:** Featuring 48 snippets of ambulatory ECG recordings spanning half an hour each from 47 subjects across five heart conditions [16, 7]. The samples, originally recorded at 125Hz, have been adjusted to 144 in length for U-Net compatibility. The training set has 87554 samples, with the majority class having 72471 samples and the smallest class having 641. The test set includes 21892 samples, ranging from 162 to 18118 samples per class, again underlining the dataset’s imbalance.

For an in-depth exploration of the datasets, kindly refer to the Appendix.

4.2 Visualization of Raw Signals

To assess the fidelity of synthetic signals visually, we present a comparative plot between several real and synthetic signals. For continuity, discrete signal values at each sampling interval are interconnected. Figure 5 illustrates a set of both real and synthetic signals derived from three distinct datasets. An immediate examination reveals the capability of our diffusion model in crafting synthetic signals that closely mirror the genuine signals.

4.3 Projection Through Dimension Reduction

For each class in every dataset, an unconditional diffusion model is trained. The UMAP projection of synthetic signals in relation to the original ones for select data classes is depicted in Figure 6. Extended visualizations are accessible in the provided source code repository. When scrutinized, it becomes evident that even for signals of considerable length (e.g., 512 timesteps), our diffusion model adeptly recognizes and replicates the intricate signal patterns. Moreover, the synthetic signals span the entire feature spectrum inhabited by the genuine signals.

4.4 Similarity Metrics and Results

The label-conditional diffusion model not only emulates the synthetic signal generation prowess of the unconditional model but also provides a guided synthesis tailored for specific classes. While the raw signals and UMAP projections closely resemble the ones in Figures 5 and 6, the main advantage lies in the training

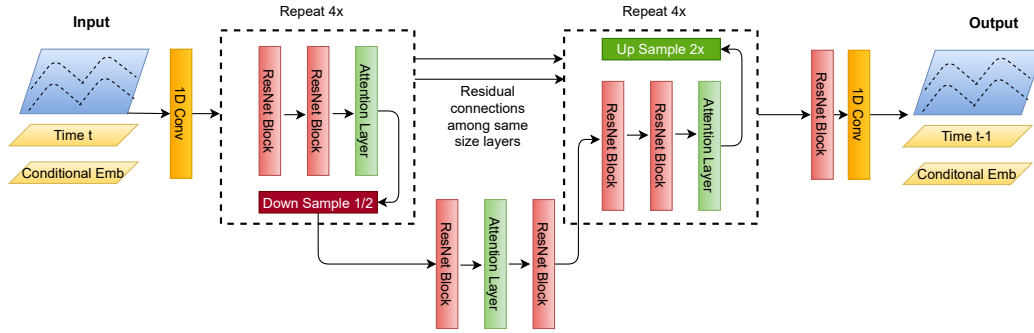


Figure 4: Description of the U-Net architecture for signals with skip connections

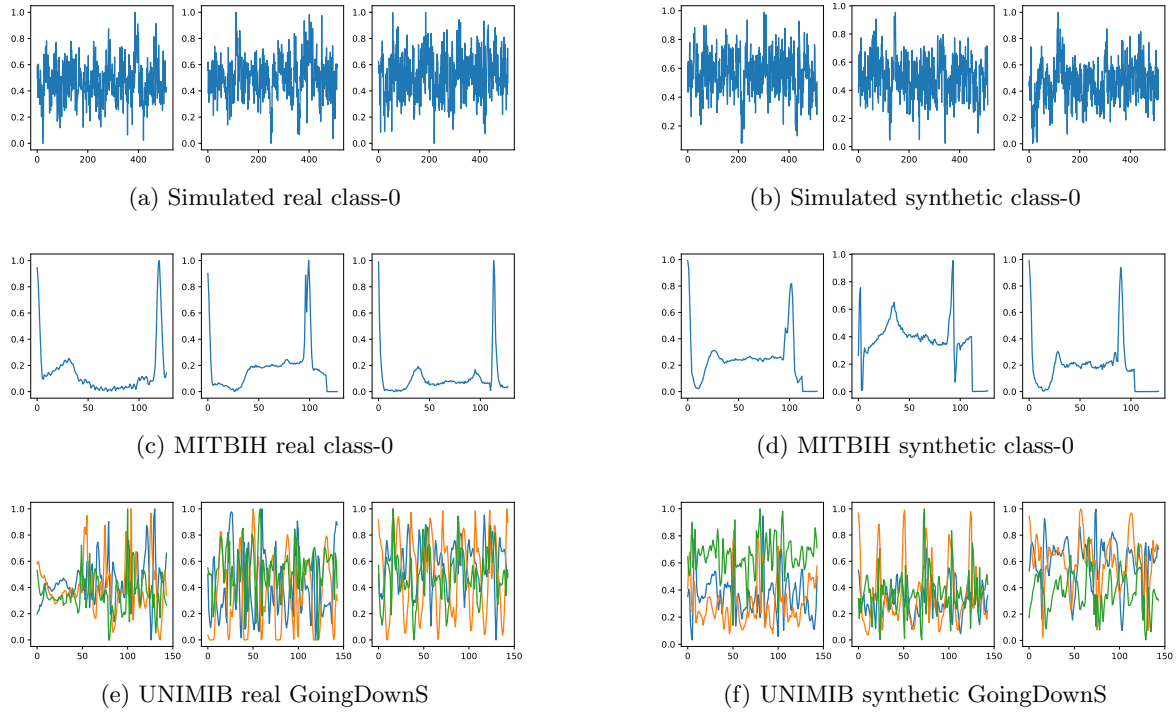


Figure 5: Raw signals comparison. The left column shows real raw signals. The right column shows synthetic raw signals.

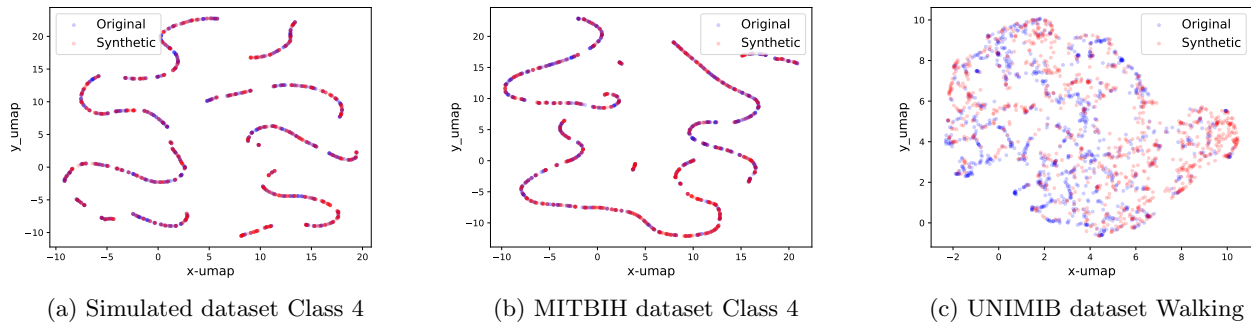


Figure 6: The real and synthetic data UMAP projection on three classes of three datasets. Each red dot represents one original signal after the dimension reduction, whereas a blue dot represents one synthetic signal. From the graphs, we can see that a set of synthetic signals are having similar distribution as a set of real signals in the 2D UMAP projections graphs.

efficiency. A singular label-conditional diffusion model suffices for a multi-class dataset, in contrast to the multiple models required by the unconditional counterpart for each class. Intriguingly, when it comes to sparsely represented data classes, the label-conditional model potentially outperforms the unconditional one. This edge is attributed to its capacity to generalize patterns across the dataset and utilize this knowledge for class-specific synthesis.

To underscore the fidelity of signals generated by our diffusion models, we calculate similarity scores across diverse signal classes. The results are cataloged in Table 1. Our BioDiffusion model’s outputs closely align with real signals, surpassing the fidelity of other cutting-edge techniques.

Quantitative Metrics:

- **Wavelet Coherence:** A measure to assess common oscillations between two time-series across specific frequencies over time. Values oscillate between 0 and 1, with 1 denoting impeccable coherence. Due to its proficiency with non-stationary signals, it’s a vital tool for evaluating evolving spectral content [11].
- **Discriminative Score:** Conceived as a quantitative metric to juxtapose sequences from real and generated datasets. It employs a 2-layer LSTM classifier trained to segregate the two datasets. The classification error on a separate test set offers an objective similarity evaluation [28].

Baseline Techniques:

- **C-RNN-GAN:** A pioneering GAN-based solution for sequential data synthesis using two-layer LSTM for both generator and discriminator [15].
- **RCWGAN:** An enhanced version of C-RNN-GAN with conditional data input for controlled generation [2].
- **TimeGAN:** A groundbreaking GAN framework that harnesses a latent space for time-series synthesis, augmented with both supervised and unsupervised losses [28].
- **SigCWGAN:** Enhances the GAN process with conditional data and the Wasserstein loss for stable training [17].
- **TTS-GAN:** A novel transformer-centric GAN model focusing on high-fidelity single-class time-series generation [11].
- **TTS-CGAN:** An iterative version of TTS-GAN introducing a label conditional transformer GAN,

Table 1: Comparison scores of real and synthetic data generated by different state-of-the-art time-series generation models.

Wavelet Coherence score (the higher the better)				
Models	SittingDown	Jumping	Non-Ectopic	FusionBeats
C-RNN-GAN	41.10	40.29	30.44	25.51
RCWGAN	39.90	38.85	29.72	22.97
TimeGAN	40.45	39.42	31.55	21.98
SigCWGAN	41.60	41.02	31.36	22.87
TTS-GAN	43.92	47.64	45.30	55.64
TTS-CGAN	45.07	47.64	47.79	58.34
BioDiffusion	78.17	90.30	89.30	91.81
Discriminative score (the lower the better)				
Models	SittingDown	Jumping	Non-Ectopic	FusionBeats
C-RNN-GAN	0.308	0.304	0.189	0.493
RCWGAN	0.294	0.311	0.483	0.499
TimeGAN	0.261	0.217	0.464	0.312
SigCWGAN	0.310	0.308	0.413	0.491
TTS-GAN	0.294	0.167	0.107	0.380
TTS-CGAN	0.191	0.057	0.162	0.261
BioDiffusion	0.126	0.121	0.159	0.231

facilitating multi-class synthesis through a singular model [12].

4.5 Utility of Synthetic Signals in Addressing Class Imbalance

To explore the potential of synthetic signals in rectifying class imbalance issues, we constructed a classification experiment centered around the MIT-BIH dataset. This dataset, while demonstrating commendable overall accuracy, manifests stark class imbalances, often disadvantaging minority classes in terms of precision and recall.

Experimental Setup: Initially, a 1D-CNN classification model was trained on the MIT-BIH training set. Given the inherent class disparities, minority classes recorded suboptimal precision and recall metrics, adversely influenced by dominant classes. Subsequently, we employed our label diffusion model to generate synthetic signals for each class. These synthetic signals were incorporated into the training set, striving to alleviate the dataset’s imbalance. The identical classification model was retrained and then assessed using the same genuine test set. For a comprehensive evaluation, our method’s performance was juxtaposed against traditional resampling techniques and other generative models employed for signal synthesis.

Results and Analysis: As presented in Table 2, synthetic signals crafted using our BioDiffusion model not only enhanced the training set but also significantly bolstered the F1-score for the detection of minority classes. In contrast, signals synthesized by models like RCWGAN and C-RNN-GAN led the downstream classifier to a biased classification—predominantly towards the majority class (Non-Ectopic Beats), effectively nullifying the F1-score for other classes. It is

Table 2: Per-class F1-scores for MIT-BIH classification, using synthetic data to mitigate class imbalance. Abbreviations: N-Ect = Non-Ectopic Beats, S-Ect = Supraventricular Ectopic Beats, Vent = Ventricular Beats, Unk = Unknown Beats, Fus = Fusion Beats.

	N-Ect	S-Ect	Vent	Unk	Fus	Average
Imbalanced	0.97	0.25	0.75	0.38	0.89	0.648
Re-sampling	0.50	0.65	0.64	0.81	0.85	0.69
TimeGAN	0.60	0.48	0.75	0.48	0.93	0.648
SigCWGAN	0.59	0.60	0.80	0.58	0.93	0.7
TTS-GAN	0.60	0.77	0.75	0.60	0.91	0.726
TTS-CGAN	0.66	0.78	0.77	0.85	0.93	0.798
BioDiffusion	0.73	0.79	0.86	0.84	0.95	0.834

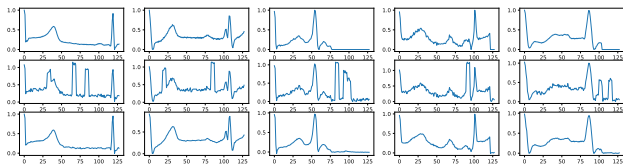


Figure 7: Example signal denoising results. First row: real signals. Second row: signals with noise. Third row: denoised signals using BioDiffusion.

pivotal to note that during these evaluations, the real test set remained untouched and unseen throughout all generative model training phases.

4.6 BioDiffusion for in Biomedical Signal Denoising, Imputation, and Upsampling

In time-series signal collections, three predominant noise types are frequently encountered: thermal noise, electrode contact noise, and motion artifacts. Thermal noise arises from the thermal agitation of electrons causing voltage or current fluctuations. Electrode contact noise stems from the changing electrical characteristics between electrodes and surfaces leading to signal baseline fluctuations. Motion artifacts, on the other hand, are sudden spikes in signals due to physical disturbances like movement, unrelated to the actual biological activity being measured. These artifacts and noise types challenge the robustness of

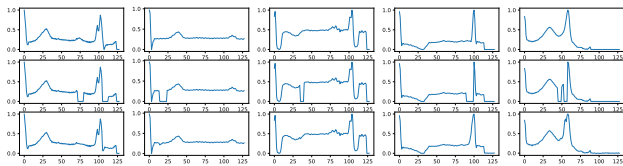


Figure 8: Example signal imputation results. First row: real signals. Second row: signals with random blanks. Third row: imputed signals by BioDiffusion model.

signal processing techniques. Leveraging BioDiffusion, we successfully denoised signals by taking the MIT-BIH dataset, adding artificial noise, and using it as an input for the diffusion model.

Furthermore, BioDiffusion efficiently handles signal imputation tasks. Missing values in collected signals can be interpolated using our model, resulting in reconstructed signals that are impressively close to the original signals, as displayed in Fig. 14.

Differing sampling rates across biomedical signals, due to equipment variations, necessitate resampling techniques. Traditional upsampling methods, while functional, often fail to capture intricate relationships among signal features. This problem is addressed with our signal conditional diffusion model designed for signal upsampling, resulting in high-resolution signals that are almost indistinguishable from the originals.

A notable application of BioDiffusion lies in the generation of individualized signals. Scarcity of data samples from individual subjects can be a bottleneck for certain machine learning applications. However, our approach allows a diffusion model to be trained on diverse signals, which is then fine-tuned using signals from an individual subject. This method generates synthetic signals that retain the unique patterns of the subject, enabling the expansion of subject-specific datasets.

For more visual examples of the output of BioDiffusion in upsampling and personalized signal generation, please see the Appendix.

5 Conclusion

In conclusion, the proposed BioDiffusion model is a novel and versatile probabilistic model specifically designed for generating synthetic biomedical signals. Our model offers a comprehensive solution for various generation tasks, including unconditional, label-conditional, and signal-conditional generation, which makes it a valuable tool for biomedical signal synthesis. We evaluated the quality of the generated signals using qualitative and quantitative assessments and demonstrated the effectiveness and accuracy of the BioDiffusion model in producing high-quality synthetic biomedical signals. Compared to state-of-the-art time-series synthesis models, our BioDiffusion model consistently outperforms its counterparts, showcasing its superiority and robustness in biomedical signal generation. The model’s versatility and adaptability have the potential to significantly contribute to the advancement of biomedical signal processing techniques, opening up new possibilities for improved research outcomes and clinical applications.

References

- [1] Juan Miguel Lopez Alcaraz and Nils Strodthoff. Diffusion-based time series imputation and forecasting with structured state space models. *arXiv preprint arXiv:2208.09399*, 2022.
- [2] Cristóbal Esteban, Stephanie L Hyland, and Gunnar Rätsch. Real-valued (medical) time series generation with recurrent conditional gans. *arXiv preprint arXiv:1706.02633*, 2017.
- [3] Vincent Fortuin, Gunnar Rätsch, and Stephan Mandt. Multivariate time series imputation with variational autoencoders. *arXiv preprint arXiv:1907.04155*, 67, 2019.
- [4] Biying Fu, Florian Kirchbuchner, and Arjan Kuijper. Data augmentation for time series: Traditional vs generative models on capacitive proximity time series. In *Proceedings of the 13th ACM International Conference on Pervasive Technologies Related to Assistive Environments, PETRA '20*, New York, NY, USA, 2020. Association for Computing Machinery.
- [5] Ankush Ganguly and Samuel WF Earp. An introduction to variational inference. *arXiv preprint arXiv:2108.13083*, 2021.
- [6] Olivier Garnier, Grant M. Rotskoff, and Eric Vanden-Eijnden. Diffusion generative models in infinite dimensions. *arXiv preprint arXiv:2212.00886*, 2023.
- [7] Ary L Goldberger, Luis AN Amaral, Leon Glass, Jeffrey M Hausdorff, Plamen Ch Ivanov, Roger G Mark, Joseph E Mietus, George B Moody, Chung-Kang Peng, and H Eugene Stanley. Physiobank, physiotoolkit, and physionet: components of a new research resource for complex physiologic signals. *circulation*, 101(23):e215–e220, 2000.
- [8] Jonathan Ho, Ajay Jain, and Pieter Abbeel. Denoising diffusion probabilistic models. *Advances in Neural Information Processing Systems*, 33:6840–6851, 2020.
- [9] Mohammad Kachuee, Shayan Fazeli, and Majid Sarrafzadeh. Ecg heartbeat classification: A deep transferable representation. In *2018 IEEE international conference on healthcare informatics (ICHI)*, pages 443–444. IEEE, 2018.
- [10] Zhifeng Kong, Wei Ping, Jiaji Huang, Kexin Zhao, and Bryan Catanzaro. Diffwave: A versatile diffusion model for audio synthesis. *arXiv preprint arXiv:2009.09761*, 2020.
- [11] Xiaomin Li, Vangelis Metsis, Huangyingrui Wang, and Anne Hee Hiong Ngu. Tts-gan: A transformer-based time-series generative adversarial network. In *Artificial Intelligence in Medicine: 20th International Conference on Artificial Intelligence in Medicine, AIME 2022, Halifax, NS, Canada, June 14–17, 2022, Proceedings*, pages 133–143. Springer, 2022.
- [12] Xiaomin Li, Anne Hee Hiong Ngu, and Vangelis Metsis. Tts-cgan: A transformer time-series conditional gan for biosignal data augmentation. *arXiv preprint arXiv:2206.13676*, 2022.
- [13] Leland McInnes, John Healy, and James Melville. Umap: Uniform manifold approximation and projection for dimension reduction. *arXiv preprint arXiv:1802.03426*, 2018.
- [14] Daniela Micucci, Marco Mobilio, and Paolo Napolitano. Unimib shar: A dataset for human activity recognition using acceleration data from smartphones. *Applied Sciences*, 7(10), 2017.
- [15] Olof Mogren. C-rnn-gan: Continuous recurrent neural networks with adversarial training. *arXiv preprint arXiv:1611.09904*, 2016.
- [16] George B Moody and Roger G Mark. The impact of the mit-bih arrhythmia database. *IEEE Engineering in Medicine and Biology Magazine*, 20(3):45–50, 2001.
- [17] Hao Ni, Lukasz Szpruch, Magnus Wiese, Shujian Liao, and Baoren Xiao. Conditional sigwasserstein gans for time series generation. *arXiv preprint arXiv:2006.05421*, 2020.
- [18] Aaron van den Oord, Sander Dieleman, Heiga Zen, Karen Simonyan, Oriol Vinyals, Alex Graves, Nal Kalchbrenner, Andrew Senior, and Koray Kavukcuoglu. Wavenet: A generative model for raw audio. *arXiv preprint arXiv:1609.03499*, 2016.
- [19] Robin Rombach, Andreas Blattmann, Dominik Lorenz, Patrick Esser, and Björn Ommer. High-resolution image synthesis with latent diffusion models, 2021.
- [20] Charissa Ann Ronao and Sung-Bae Cho. Human activity recognition with smartphone sensors using deep learning neural networks. *Expert systems with applications*, 59:235–244, 2016.
- [21] Yannick Roy, Hubert Banville, Isabela Albuquerque, Alexandre Gramfort, Tiago H Falk, and Jocelyn Faubert. Deep learning-based electroencephalography analysis: a systematic review.

Journal of neural engineering, 16(5):051001, 2019.

- [22] Chitwan Saharia, Jonathan Ho, William Chan, Tim Salimans, David J Fleet, and Mohammad Norouzi. Image super-resolution via iterative refinement. *IEEE Transactions on Pattern Analysis and Machine Intelligence*, 2022.
- [23] Jascha Sohl-Dickstein, Eric Weiss, Niru Maheswaranathan, and Surya Ganguli. Deep unsupervised learning using nonequilibrium thermodynamics. In *International Conference on Machine Learning*, pages 2256–2265. PMLR, 2015.
- [24] Yang Song and Stefano Ermon. Improved techniques for training score-based generative models. *Advances in neural information processing systems*, 33:12438–12448, 2020.
- [25] Yusuke Tashiro, Jiaming Song, Yang Song, and Stefano Ermon. CSDI: Conditional score-based diffusion models for probabilistic time series imputation. *Advances in Neural Information Processing Systems*, 34:24804–24816, 2021.
- [26] Unite.AI. Diffusion models in ai – everything you need to know, 2021.
- [27] Ling Yang, Zhilong Zhang, Yang Song, Shenda Hong, Runsheng Xu, Yue Zhao, Wentao Zhang, Bin Cui, and Ming-Hsuan Yang. Diffusion models: A comprehensive survey of methods and applications. *arXiv preprint arXiv:2209.00796*, 2022.
- [28] Jinsung Yoon, Daniel Jarrett, and Mihaela Van der Schaar. Time-series generative adversarial networks. *Advances in neural information processing systems*, 32, 2019.

A Dataset details

More of the dataset details is in Table 3

Table 3: Dataset details

Dataset	Signal type	N Channels	Type	Total samples	Classes	Class ratio	Sample length
Simulated	Simulated signals	1	Train	20000	5	1:1:1:1:1	512
		1	Test	2000	5	1:1:1:1:1	512
UNIMIB	Accelerometer signals	3	Train	6055	9	119:169:1394: 1572:737:600: 1068:228:168	128
		3	Test	1524	9	34:47:344: 413:184:146: 256:68:32	128
MITBIH	ECG signals	1	Train	87554	5	72471:2223: 5788:641:6431	144
		1	Test	21892	5	18118:556: 1448:162:1608	144

B Training details

We train an unconditional diffusion model per class per dataset. The training details are as follows.

Architecture

- Base channels: 64
- Channel multipliers: 1, 2, 4, 8, 8 (Simulated Dataset)
- Channel multipliers: 1, 2, 4, 8 (UNIMIB and MITBIH)
- Residual blocks groups: 8
- Attention heads: 4

Training

- Optimizer: Adam
- Batch size: 32
- Learning rate: 3e-4
- Epochs: 100
- Hardware: NVIDIA RTX A5000

Diffusion

- Timesteps: 1000
- Noise schedule: cosine
- Loss: l1

We train a label condition diffusion model per dataset. Each signal sample is paired with a scalar label. The training details are as follows.

Architecture

- Base dimensions: 64
- Channel multipliers: 1, 2, 4, 8, 8 (Simulated Dataset)
- Channel multipliers: 1, 2, 4, 8 (UNIMIB and MITBIH)
- Number classes: 5 (Simulated and MITBIH dataset)
- Number classes: 9 (UNIMIB dataset)
- Residual blocks groups: 8

- Attention heads: 4

Training

- Optimizer: Adam
- Batch size: 32
- Learning rate: 3e-4
- Epochs: 100
- Hardware: NVIDIA GeForce 1080
- Conditional drop prob: 0.5

Diffusion

- Diffusion timesteps: 1000
- Loss: l1
- Noise schedule: cosine

A signal conditional model is trained on a specific class of data, and synthetic signals are generated by using distorted signals as conditional inputs. The distorted signals provided to the model were not present in the training set, with the aim of assessing the model’s ability to accurately restore them to their original form. Here we present several possible implementations of the model, it should be noted that these examples are not exhaustive, and the model is capable of other implementations as well.

Architecture

- Base channels: 64
- Channel multipliers: 1, 2, 4, 8, 8
- Residual blocks groups: 2
- Attention heads: 4

Training

- Optimizer: Adam
- Batch size: 32
- Learning rate: 1e-4
- iterations: 1000000
- Hardware: NVIDIA GeForce 1080

Diffusion

- Timesteps: 2000
- Noise schedule: linear
- Loss: l1

C More visualizations about label conditional generation

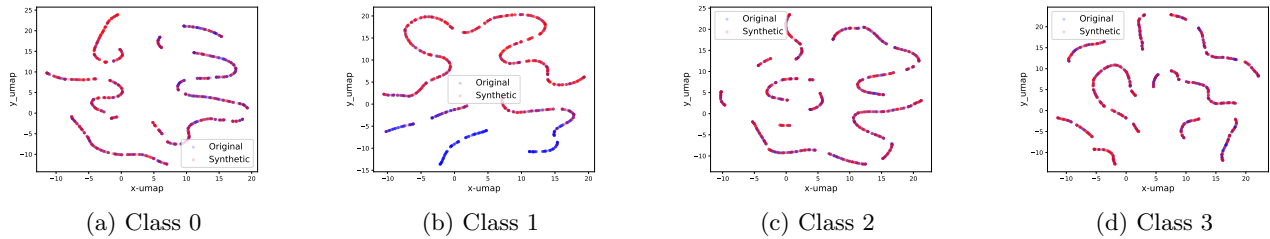


Figure 9: Real and synthetic signal UMAP projection on selected classes of simulated dataset

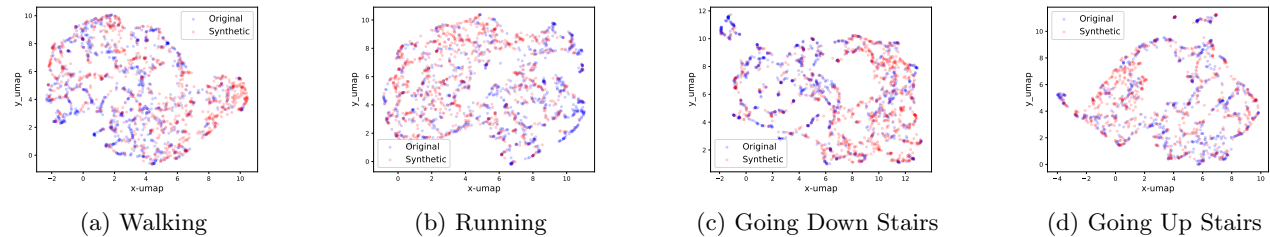


Figure 10: Real and synthetic signal UMAP projection on selected classes of UniMiB dataset

D More visualizations about signal conditional generation

D.1 Signal Denoising

We selected three types of noise that are frequently involved in time-series signal collections. They are:

- **Thermal noise**, also known as white noise, is a type of random electrical noise that occurs in electronic circuits and arises from the thermal agitation of electrons, which results in a fluctuation of the voltage or current that is independent of the signal being measured.

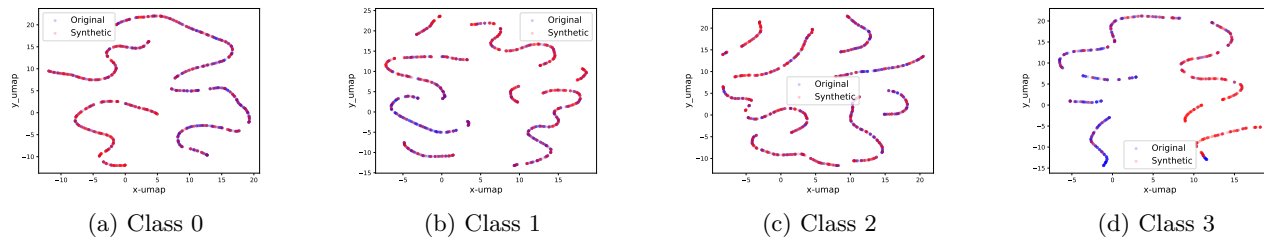


Figure 11: Real and synthetic signal UMAP projection on selected classes of MITBIH ECG dataset

- **Electrode contact noise**, also known as low-frequency drift, is a type of noise that arises in electronic measurements due to changes in the electrical characteristics of the contact between the electrode and the surface being measured, which can cause fluctuations in the baseline signal over time.
- **Motion artifacts**, also known as random spikes, are unwanted signals that can occur in physiological or biological measurements due to movement or other physical disturbances, which can cause sudden, brief spikes in the recorded signal that are not related to the underlying biological activity being measured.

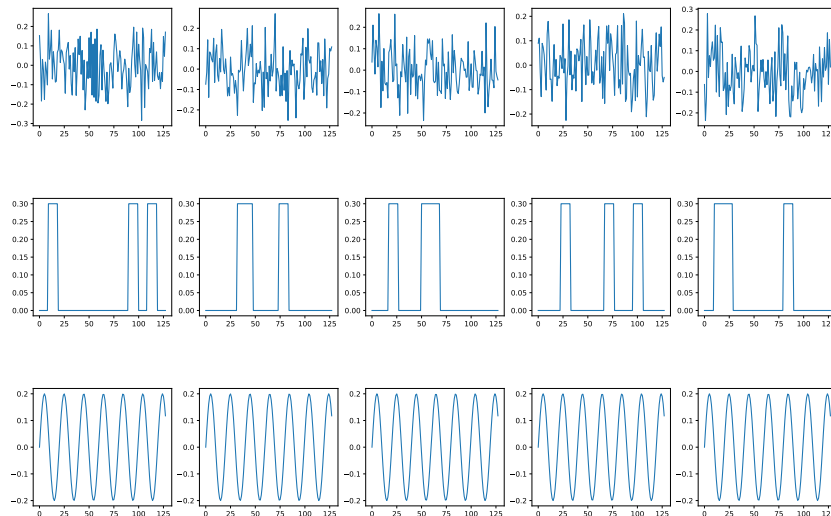


Figure 12: Three type of noises involved in biomedical signals. First row: Thermal noise. Second row: Motion artifacts noise Third row: Electrode noise

Fig.12 shows some random noise examples. We intentionally distort the signals with such noise to make them as signal condition input to the diffusion models. The Fig. 13 shows how BioDiffusion can help remove signal artifacts. The top row shows some real signals from the MITBIH dataset. The middle row shows the same signals with added artificial noise. They are the input to the diffusion model. The bottom row shows the generated synthetic signals, which ideally should be as much as the top row signals. Please note that these signals are from the MITBIH testing set, which are unseen when training the signal conditional diffusion model.

D.2 Signal Imputation

Signal imputation is another task that BioDiffusion can handle. Oftentimes, the collected signals may contain some missing values. We can use BioDiffusion to fill in those blanks. Fig. 14 shows a few examples of signal imputation. The first row shows the original signals. The second row shows the same signals with some randomly missing values (values set to zero). We use them as signal conditions input to the diffusion model. The third row shows the reconstructed signals. We can see that the synthetic signals fill in the blanks and are very similar to the original signals.

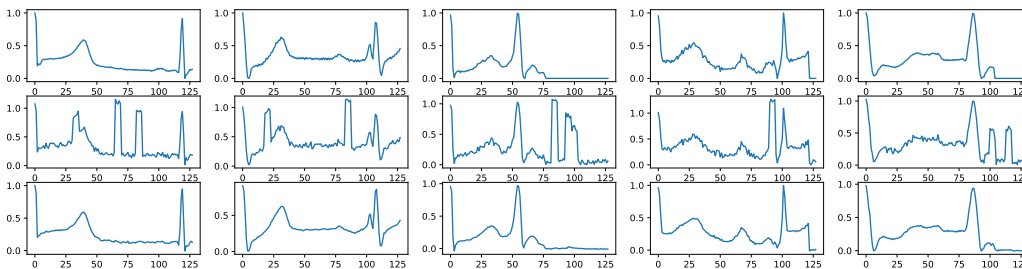


Figure 13: Example signal denoising results. First row: real signals. Second row: signals with noise. Third row: denoised signals using BioDiffusion.

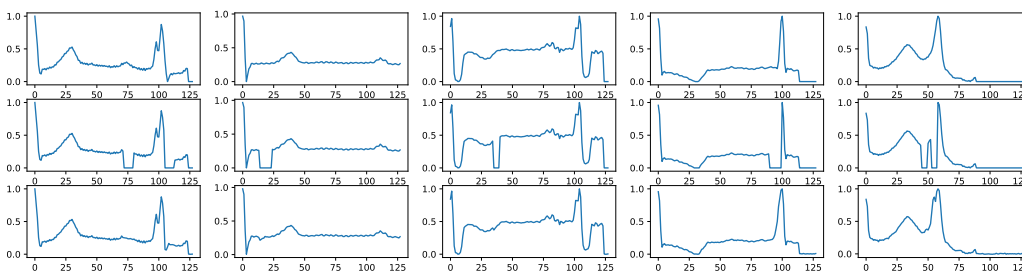


Figure 14: Example signal imputation results. First row: real signals. Second row: signals with random blanks. Third row: imputed signals using BioDiffusion.

D.3 Signal Super-resolution

Biomedical signals of identical types can possess distinct sampling rates due to the usage of different equipment for collection. This necessitates the application of signal downsampling or upsampling techniques to match the sampling rates when these signals are used concurrently. However, conventional upsampling methods like Hamming windows, linear/cubic interpolation, and zero-padding followed by low-pass filtering, may fall short in capturing intricate relationships among signal features. This shortcoming restricts their capacity to generate high-quality, realistic upsampled signals. A potential solution to this limitation can be found in deep learning-based super-resolution techniques. Our signal conditional diffusion model, designed for signal upsampling, has been trained to create high-resolution signals that closely resemble their original counterparts. This is illustrated in Fig 15, where the model-generated signal exhibits features more akin to the original signal than the downsampled version.

D.4 Individual signal generation

One of the challenges that hinders certain machine learning applications on biomedical signals is the insufficient data samples from each individual subject. To address this issue, signal conditional diffusion models can be utilized. Initially, a diffusion model is trained on a specific type of signals from numerous subjects. Afterwards, a small number of signals from a single subject are utilized as conditional inputs to enable the diffusion model to generate a multitude of synthetic signals that incorporate the distinctive data patterns of that subject. As a result, synthetic signals can be employed to expand the dataset size of an individual subject and facilitate the development of machine learning applications tailored to that particular subject.

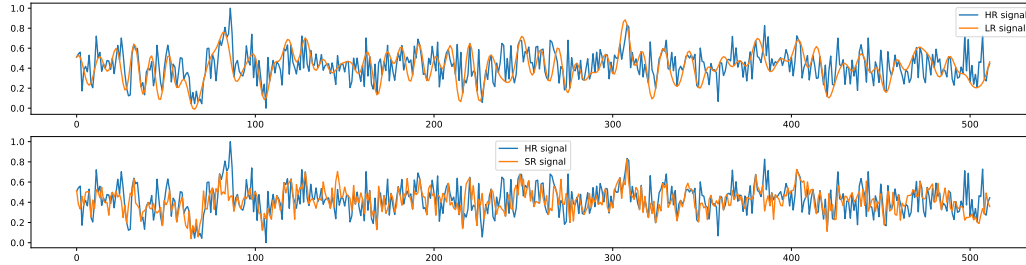


Figure 15: This figure provides an example of signal super-resolution results, where the blue lines represent one of the original signals with 512 timesteps, the upper graph orange line shows the signal downsampled to 1/4 and then upsampled to 512 timesteps using the Scikit-Learn ‘resample()’ method, and the bottom graph orange line shows the super-resolution signal generated by the diffusion model using the downsampled signal as conditional input.

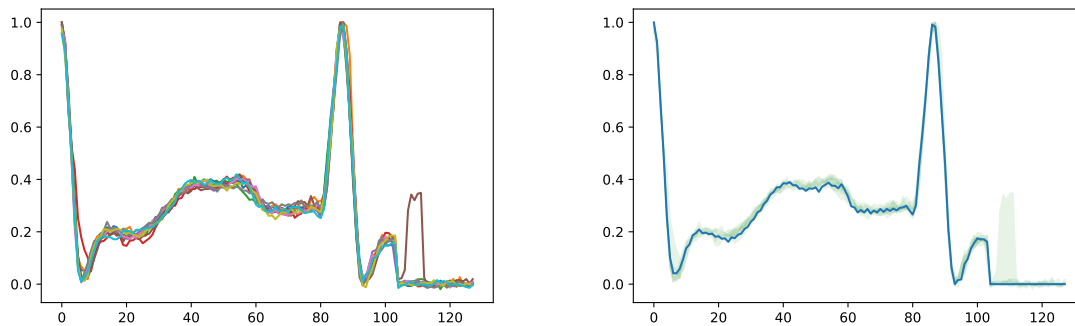


Figure 16: Generated synthetic heartbeat signals from a single real signal. The left graph shows 10 synthetic signals. In the right graph, the blue line represents the original signal, and the green area shows the value range of the 10 synthetic signals.